

## Nanostructure and Composition Control of Fluorocarbon Films from Modulated Tetrafluoroethylene Plasmas

G. Cicala,\* A. Milella, F. Palumbo, P. Rossini, P. Favia, and R. d'Agostino

*Istituto di Metodologie Inorganiche e dei Plasmi, CNR, Sezione di BARI, Dipartimento di Chimica-Università di Bari, Via Orabona, 4, 70126 Bari, Italy*

Received April 18, 2002

Revised Manuscript Received October 4, 2002

The deposition of thin films by PECVD (plasma enhanced chemical vapor deposition) technique from tetrafluoroethylene and other fluorinated monomers has been investigated with great interest in the past.<sup>1</sup> In most cases, the plasma excitation has been obtained with continuous wave (CW) discharges and the resultant CW films exhibited interesting chemical and physical properties which can be tailored by changing the conventional plasma parameters such as pressure, power, feed, flow rate, substrate temperature, and reactor geometry. The fluorocarbon films obtained in CW conditions are usually cross-linked, amorphous, and smooth when deposited in the glow region of the discharge, while the deposition of rough, thin, surface-structured, and monomer-retaining coatings has been reported in the afterglow region.<sup>2</sup> Processes, plasma diagnostics, and surface characterization of CW fluorocarbon films have been deeply investigated, and an ion-bombardment activated growth mechanism (AGM) has been accepted.<sup>1</sup>

PECVD and other plasma processes have been investigated also in modulated discharges (MD) and it has been found that modulating the discharge (i.e., switching periodically on–off) can improve the control of the process for both the plasma phase<sup>3,4</sup> and the deposited films.<sup>5–7</sup> Recent studies on MD coatings show that many issues related to their structure and deposition mechanism are still unsolved.

In this communication, we report that MD films, deposited from tetrafluoroethylene (TFE, C<sub>2</sub>F<sub>4</sub>) under selected modulation conditions, exhibit marked surface structures (morphology) on the nanoscale, as well as monomer retention, i.e., a composition very similar to poly(tetrafluoroethylene) (PTFE or Teflon). We remark that MD plasmas, contrary to CW ones, afford an important and innovative tool to tune the formation of the growth precursors, and correspondingly, the composition, the structure and the morphology of the resultant films. It is worthy noticing that generally, PTFE-like films exhibit interesting hydrophobic features (water contact angles 95–115°). However, our MD films show a very unusual super-hydrophobicity (water contact angles ≥160°) determined by the combined action of the morphology (nanostructure) and the composition (high F/C ratio). Such a material can find many important applications, e.g., for stain resistant clothes, self-cleaning surfaces, nonfouling substrates, etc.

In the present paper, we examine the effect of the duty cycle on the time-resolved CF<sub>2</sub><sup>\*</sup> emitting species in MD C<sub>2</sub>F<sub>4</sub> plasmas and on the composition and morphol-

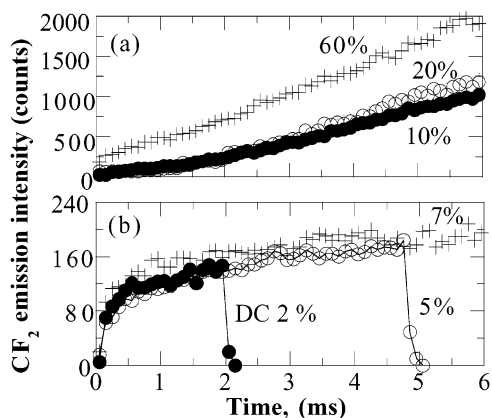
ogy of the deposited CF<sub>x</sub> films. Films deposited in CW conditions, or at high duty cycles (≥10%), are amorphous and smooth, characterized by F/C ratio values decreasing as a function of the duty cycle. When a low duty cycle (<10%) is utilized, the film features a high F/C ratio and a crystalline character, with neat surface ribbonlike structures. The two different deposition regimes can be distinguished by time-resolved optical emission spectroscopy (TROES) of CF<sub>2</sub><sup>\*</sup> species, which exhibit very different trends in the on time period, as it will be shown later. The process is performed in a quartz tubular reactor (8 cm in diameter and 50 cm in length) in a quasi parallel plate configuration, with an external electrode capacitively coupled via a matching network to an rf (13.56 MHz) generator and an internal grounded electrode. While the external electrode is conformal with the quartz tube, the internal one is flat. In MD conditions, the rf generator has been coupled to a square wave pulse generator with variable modulation period, ( $P = \text{time}_{\text{on}} + \text{time}_{\text{off}}$ ) and duty cycle, ( $DC = \text{time}_{\text{on}} / (\text{time}_{\text{on}} + \text{time}_{\text{off}}) \times 100$ ). Power, pressure, substrate temperature, C<sub>2</sub>F<sub>4</sub> flow rate, and deposition time have been kept constant at 30 W, 300 mTorr, room temperature, 6 sccm, and 90 min, respectively, whereas the modulation parameters have been varied: the period from 20 to 200 ms and the duty cycle from 2 to 100% (CW). It is important to consider that the effective power delivered depends on the DC, according to

$$W_{\text{eff}} = W_{\text{tot}} DC$$

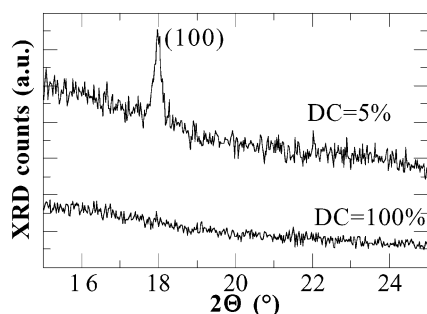
For this short communication, we report only the 100 ms period results at various duty cycles. Thin fluorocarbon films have been deposited on silicon substrates placed onto the grounded electrode. Optical emission spectroscopy (OES) has been used to monitor the excited species generated in CW plasma, whereas TROES has been used to detect the emission signals during the modulation period. In the TROES acquisition mode the spectroscopy (optical multichannel analyzer EG&G-PAR OMALIII) has been synchronized by the square pulse generator, as in ref 3. OES spectra of C<sub>2</sub>F<sub>4</sub> plasmas denote the dominant presence of the CF<sub>2</sub><sup>\*</sup> species; the emissions are principally due to the transition of the A<sup>1</sup>B<sub>1</sub>–X<sup>1</sup>A<sub>1</sub> (230–340 nm) and <sup>3</sup>B<sub>1</sub>–<sup>1</sup>A<sub>1</sub> (340–450 nm) systems.<sup>8</sup> CF<sup>\*</sup> radical and F<sup>\*</sup> atom are not observed as already found in refs 1, 9, and 10. Among the numerous overlapped bands of CF<sub>2</sub><sup>\*</sup>, the band centered at 340.8 nm has been considered for the present study. A small quantity of Ar has been added and the emission line at 750 nm has been followed. The chemical composition, the crystallinity and the morphology of the deposited fluorocarbon films have been determined by Fourier transform IR spectroscopy (FTIR), X-ray photoelectron spectroscopy (XPS), X-ray diffractometry (XRD), and scanning electron microscopy (SEM), respectively. Data of plasma phase and results of film characterization will be presented and discussed.

Figure 1 shows the time-resolved CF<sub>2</sub><sup>\*</sup> emission intensity detected in MD mode. The period is held constant at a value of 100 ms, whereas the duty cycle values are varied. The figure is split in two for allowing the different intensity scales of CF<sub>2</sub><sup>\*</sup> emission.

\* Corresponding author. E-mail: cicala@area.ba.cnr.it.



**Figure 1.** Time evolution of  $\text{CF}_2^*$  emission intensities (340.8 nm) in modulated  $\text{C}_2\text{F}_4$  plasmas at fixed period of 100 ms and duty cycle values (a) of 10, 20, 60% and (b) of 2, 5, and 7%.



**Figure 2.** XRD patterns of  $\text{CF}_x$  films (deposited on crystalline silicon) obtained by modulated  $\text{C}_2\text{F}_4$  plasmas at different duty cycle values 5 and 100% and fixed period of 100 ms.

The data at higher DCs and consequently at higher  $W_{\text{eff}}$  are reported in Figure 1a, while the curves obtained with DCs  $\leq 7\%$  and lower  $W_{\text{eff}}$  are shown in Figure 1b. There are a few considerations which can be made by the inspection of the figure, namely, the following:

1. At low  $W_{\text{eff}}$  and DC,  $\text{CF}_2^*$  intensity increases up to 1 ms and then is saturated at higher times.
2. At higher  $W_{\text{eff}}$  and DC  $\geq 10\%$ ,  $\text{CF}_2^*$  intensity is much higher and continuously increases.
3. The  $\text{CF}_2^*$  intensity exhibits increasing values at zero time as the DC increases.

Under the same conditions, the Ar intensity is constant; hence, the electron density does not vary with the on time.

IR spectra of fluorocarbon films, grown at various decreasing DC values (100–5%) and reported in ref 11 show the following evolution: (1) the disappearance of the unsaturated bonds  $\text{>C=C<}$  at  $1718\text{--}1780\text{ cm}^{-1}$ ; (2) the narrowness of the strong absorption of  $\text{CF}_x$  ( $x = 1, 2, 3$ ) groups extending from  $980$  to  $1550\text{ cm}^{-1}$  and an increasing resolution of peaks at  $1160$  and  $1220\text{ cm}^{-1}$  due to the symmetric and asymmetric stretching modes of  $\text{CF}_2$ , respectively;<sup>1</sup> (3) the decrease of the absorption band at  $740\text{ cm}^{-1}$ , known as the *amorphous band* of PTFE.<sup>12</sup> The intensity extent of this last absorption is related to the long-range order or crystallinity: the lower the absorption intensity, the higher the crystallinity. The preceding statement is corroborated by XRD measurements.

Figure 2 shows two typical XRD patterns of fluorocarbon films grown under CW mode and DC = 5%. The CW sample is amorphous, whereas the MD material is partially crystalline.

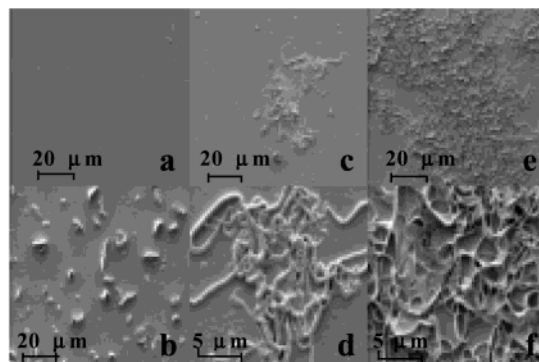


**Figure 3.** Typical scanning electron micrographs of  $\text{CF}_x$  films (deposited on crystalline silicon) obtained by modulated  $\text{C}_2\text{F}_4$  plasmas at fixed period of 100 ms and different duty cycle values: (a) 100, (b) 10, (c,d) 7, and (e,f) 5%.

**Table 1.**  $\text{CF}_3$ ,  $\text{CF}_2$ , CF, C–CF, and C–C Fractions and the F/C Ratio Calculated by the Deconvolution of High Resolution C 1s XPS Spectra of Fluorocarbon Films Obtained by Modulated Plasmas at Fixed Period,  $P = 100$  ms, and Variable Duty Cycle, DC<sup>a</sup>

$\text{CF}_x$ samples	$\text{CF}_3$ 294 eV (%)	$\text{CF}_2$ 292 eV (%)	CF 289.5 eV (%)	C–CF 287.2 eV (%)	C–C 285 eV (%)	F/C ratio
CW. DC = 100%	20.52	29.84	18.98	29.54	1.12	1.40
MD. DC = 10%	22.56	41.14	19.47	16.82	0	1.69
MD. DC = 7%	19.98	45.30	21.12	13.59	0	1.72
MD. DC = 5%	16.96	62.33	12.15	8.05	0	1.90
PTFE or Teflon	0	100	0	0	0	2.00

<sup>a</sup> The data relative to a PTFE sample is reported for comparison.

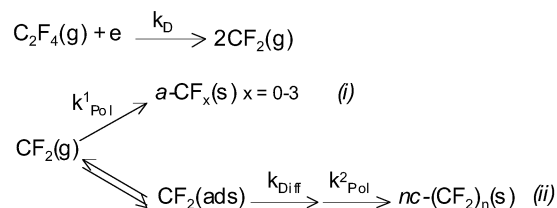
The crystallites exhibit a preferential orientation along the (100) plane of the hexagonal structure of crystalline PTFE, at  $2\theta = 18.09^\circ$ .<sup>13</sup> To authors' knowledge, this is the first report of MD films grown at room temperature exhibiting a crystalline Teflon-like matrix. Similar features have been recently obtained by W. Jiang et al.<sup>13</sup> in laser-deposited PTFE films at  $350^\circ\text{C}$ , and by S. J. Limb et al.<sup>6</sup> in pyrolytic CVD films from hexafluoropropylene oxide at  $400^\circ\text{C}$ . These last authors have found a broad shifted peak at  $2\theta = 16^\circ$  in MD film grown at room temperature.

Typical SEM images of the coatings are shown in Figure 3. The images indicate that the morphological features are absent in CW film, while neat ribbon-shaped structures appear and become highly densified in MD samples, going from 100 to 5% of DC values. These ribbon-shaped structures are many micrometers long and hundreds of nanometers wide.

The analysis of the above results evidences that the DC is a key modulation parameter because it affects strongly, on one hand, the formation kinetics of  $\text{CF}_2^*$  during the plasma on time and, on the other hand, the composition, the structure, the crystallinity, and the morphology of the resultant films. Under MD plasma conditions, the film structure becomes more ordered (see Figure 2) and from the compositional point of view leads to structure retention, and linear PTFE chains are obtained, as witnessed by infrared<sup>11</sup> and high-resolution C(1s) XPS spectra. The deconvolution of C 1s in  $\text{CF}_3$ ,  $\text{CF}_2$ , CF, C–CF, and C–C components gives the integrated areas reported in Table 1. The high  $\text{CF}_2$  fraction corresponds to a high F/C ratio of 1.9. The main features of discharge modulation with short duration of plasma on (DC  $\leq 7\%$ ) and low  $W_{\text{eff}}$  are as follows: partial

fragmentation of the monomer and low concentration of  $\text{CF}_2$ , controllable kinetics of  $\text{CF}_2^*$  species, that under our experimental conditions represent  $\text{CF}_2$  concentration in the ground state,<sup>3,14</sup> and  $\text{CF}_2$  radicals being the dominant species,<sup>1</sup> unreactive in the gas phase<sup>15</sup> and long-lived,<sup>16</sup> and establishing a particular kinetic regime accounting for the unusual film morphology.

To explain the above results the following mechanism could be hypothesized, as reported in the following scheme:



(i) High DC and  $W_{\text{eff}}$  values produce high density of radicals. The abundance of active species drives the film formation at high deposition rates inhibiting the surface migration of adsorbed species. Additionally, the higher ion bombardment can promote the cross-linking of the film.

A continuous increase of  $\text{CF}_2$  radical (see Figure 1a) in the gas phase is observed and the off time is not enough to completely remove the produced radical. In fact, at increasing DC values the  $\text{CF}_2$  emission, corresponding to on time equal to zero, increases, and this quantity is directly related to the density of  $\text{CF}_2$  survived at the end of off time of the previous pulse.

(ii) Low DC and  $W_{\text{eff}}$  values give a very low radical density, and the radicals polymerize at low deposition rate on the surface. The adsorbed  $\text{CF}_2$  radicals have enough time to diffuse on the surface to lower energy sites which become the nucleation centers for the formation of nanostructured crystalline Teflon-like ribbons.

Under these conditions, the saturation emission intensity profile can be easily explained since a stationary state of  $\text{CF}_2$  is rapidly attained due to its low amount.

In conclusion, it has been shown that the modulation of  $\text{C}_2\text{F}_4$  plasmas is a very useful tool to control the

kinetics of the heterogeneous reaction of  $\text{CF}_2$  species, considered the dominant radical,<sup>1</sup> and to shift it by tuning the duty cycle values. The amorphous to crystalline transition depends strongly on the DC values as observed by ex situ XRD and SEM and in situ TROES measurements. In particular, the TROES technique allows to determine precisely the DC critical value at which the amorphous/crystalline boundary is located.

**Acknowledgment.** The authors are grateful to Dr. G. Palumbo for his support and active participation and to Dr. M. Gazzano (CNR Bologna) for XRD measurements.

## References and Notes

- (1) d'Agostino, R.; Cramarossa, F.; Fracassi, F.; Illuzzi, F. In *Plasma Deposition, Treatment, and Etching of Polymers*; d'Agostino, R., Ed.; Academic Press: San Diego, CA, 1990; Chapter 2, pp 95–162.
- (2) Favia, P.; Perez-Luna, V. H.; Boland, T.; Castner, D. G.; Ratner, B. D. *Plasma Polym.* **1996**, *1*, 299–326.
- (3) Cicala, G.; Losurdo, M.; Capezzuto, P.; Bruno, G. *Plasma Sources Sci. Technol.* **1992**, *1*, 156–165.
- (4) Yoshida, T.; Ichikawa, Y.; Sakai, H. *Proceedings of the 9th European PV Solar Energy Conference (Freiburg)*; Palz, W., Wrixon, G. T., Helm, P., Eds.; Kluwer Academic Publisher: Dordrecht, The Netherlands, 1989; pp 1006–1009.
- (5) Chen, X.; Rajeshwar, K.; Timmons, R. B.; Chen, J.-J.; Chyan, O. M. R. *Chem. Mater.* **1996**, *8*, 1067–1077.
- (6) Limb, S. J.; Lau, K. K.; Edell, D.; Gleason, J. E. F.; Gleason, K. K. *Plasma Polym.* **1999**, *4*, 21–32.
- (7) Ryan, M. E.; Hynes, A. M.; Badyal, J. P. S. *Chem. Mater.* **1996**, *8*, 37–42.
- (8) Trung, Q. T.; Durocher, G.; Sauvageau, P.; Saudorfy, S. *Chem. Phys. Lett.* **1977**, *47*, 404–407.
- (9) d'Agostino, R.; Cramarossa, F.; Colaprico, V.; d'Ettola, R. *J. Appl. Phys.* **1983**, *54*, 1284–1288.
- (10) Millard, M. M.; Kay, E. *J. Electrochem. Soc.* **1982**, *129*, 160–165.
- (11) Favia, P.; Cicala, G.; Milella, A.; Palumbo, F.; Rossini, P.; d'Agostino, R. *Surf. Coat. Technol.*, in press.
- (12) Giegengack, H.; Hinze, D. *Phys. Status Solidi A* **1971**, *8*, 513–520.
- (13) Jiang, W.; Norton, M. G.; Tsung, L.; Dickinson, J. T. *J. Mater. Res.* **1995**, *10*, 1038–1043.
- (14) Hancock, G.; Sucksmith, J. P.; Toogood, M. J. *J. Phys. Chem.* **1990**, *94*, 3269–3272.
- (15) Dalby, F. W. *J. Chem. Phys.* **1964**, *41*, 2297–2303.
- (16) Maruyama, K.; Goto, T. *J. Phys. D* **1995**, *35*, 884–896.

MA025536E